Polymorphism

Deutsche Ausgabe: DOI: 10.1002/ange.201601022
Internationale Ausgabe: DOI: 10.1002/anie.201601022

Defect-Controlled Formation of Triclinic $Na_2CoP_2O_7$ for 4 V Sodium-Ion Batteries

Heejin Kim[+], Chan Sun Park[+], Jang Wook Choi, and Yousung Jung**

Abstract: *Simple defects such as sodium deficiencies can induce the selective synthesis of triclinic $Na_2CoP_2O_7$, providing an increase in energy density of more than 40 % compared to the stoichiometric polymorph that is preferentially formed under the commonly used synthesis conditions. Such a significant improvement, which was achieved just by changing the crystal structure, suggests that controlling the polymorphism could be an effective and facile method for developing high-performance electrode materials and that defects can play a remarkable role in this process.*

Rechargeable batteries are considered to be a key technology for energy storage systems (ESSs), yet improved electrochemical properties and reduced manufacturing costs are required for industrial applications. As a promising candidate for ESS applications, sodium ion batteries (SIBs) have recently been revisited owing to the abundance of sodium;[1] however, the energy density of SIBs is intrinsically inferior to that of lithium-ion batteries (LIBs). To obtain SIBs with a higher net energy density, several strategies have been applied to increase the cell voltage, such as fluorination,[2] transition metal (TM) alteration,[3] and polyanion modification;[4] these strategies were mostly motivated by success in related LIB studies. The structural control of polymorphism is another interesting approach to raising the cell voltage as well as to improving various electrochemical properties. Polymorphs share the same chemical formula, but their physical and chemical properties can be completely different owing to differences in the crystal structure. The electrochemical consequences of such structural differences are generally significant in electrode materials because the binding of alkali ions and the redox energy of the TM center are considerably influenced by the structure.[5]

In LIB studies, as a way of controlling the polymorphism of electrode materials, TM substitution,[6] changes in the synthesis temperature,[7] and various synthetic methods[8] have been examined. By adopting these crystal engineering approaches, various electrochemical properties such as the cell voltage[6a] and electrical conductivity[8] have been improved remarkably. These successful applications led to an investigation of the phase stabilities and different electrochemical behaviors of many different polymorphs in various electrode materials.[9] The key motivation of the present work was also to be able to design SIB cathode materials with improved energy densities by controlling the structure of the host material using defect engineering.

Disodium metal pyrophosphates ($Na_2MP_2O_7$), the focus of this paper, crystallize into seven different structures depending on the metal (M). Among these structures, the triclinic ($P\bar{1}$) polymorph, also referred to as the "rose" form because of its color, has been shown to be a promising cathode material for M = Fe.[10] The rose form of M = Mn can accommodate large structural modifications that occur during typical battery operations, such as Jahn–Teller distortions, and can provide favorable ionic migration even for M = Mn, which is otherwise difficult to activate.[3b] Later, to further increase the energy density of $Na_2MP_2O_7$, the redox center was changed from M = Fe to Co to synthesize rose $Na_2CoP_2O_7$, namely the Co rose phase; however, all reaction conditions yielded an orthorhombic (*Pna*21) polymorph, namely the Co blue phase, instead of the desired Co rose phase.[11]

In fact, the Co rose phase was first reported by Erragh et al. in 1991; the authors concluded that careful temperature control was necessary for producing rose compounds of good quality[12] (see the Supporting Information, Table S1 for the products obtained under various conditions). In their synthetic investigations, two important points were made. First, below the melting point (700 °C), the Co blue phase was preferentially formed over the Co rose phase regardless of the starting materials or the cooling rates; this is consistent with recent experiments.[11] This finding implies that the blue form is intrinsically more stable than the rose form for $Na_2CoP_2O_7$. Second, the only route to synthesize the Co rose phase was slow solidification (10 °C h^{-1}) after melting the powder at an elevated temperature of 800 °C. As a result, the Co blue and Co rose phases are separately formed at heating temperatures of 700 °C and 800 °C, respectively, even though both compounds are melted at both temperatures. In other words, heat treatments of the precursors at higher temperatures altered the relative stabilities of the Co blue and rose phases in the subsequent crystallization processes. For many syntheses of LIB cathode materials, excess amounts of the lithium precursor are often used to compensate for material loss by evaporation during heat treatment.[13] Considering that the boiling point of sodium (883 °C) is much lower than that of lithium (1342 °C), sodium can also evaporate under such high-

[*] Dr. H. Kim,[+] C. S. Park,[+] Prof. J. W. Choi, Prof. Y. Jung
Graduate School of EEWS
Korea Advanced Institute of Science and Technology
Daejeon 34141 (Republic of Korea)
E-mail: jangwookchoi@kaist.ac.kr
ysjn@kaist.ac.kr
Dr. H. Kim[+]
Suncheon Center, Korea Basic Science Institute
Suncheon 57922 (Republic of Korea)
[+] These authors contributed equally to this work.

Supporting information for this article can be found under: http://dx.doi.org/10.1002/anie.201601022.

temperature conditions. Indeed, many SIB studies have reported that owing to the volatility of sodium, an excess amount of the sodium precursor was necessary to obtain the desired materials.[14] Therefore, for the synthesis of $Na_2CoP_2O_7$, we hypothesized that a deficiency in Na content would result in the stabilization of the rose phase.

We first compared the relative stabilities of the Co rose and blue phases as a function of Na deficiency (x in $Na_{2-x}CoP_2O_7$ in Figure 1a) using electronic-structure calculations.[15] For the stoichiometric composition ($x=0$), the blue

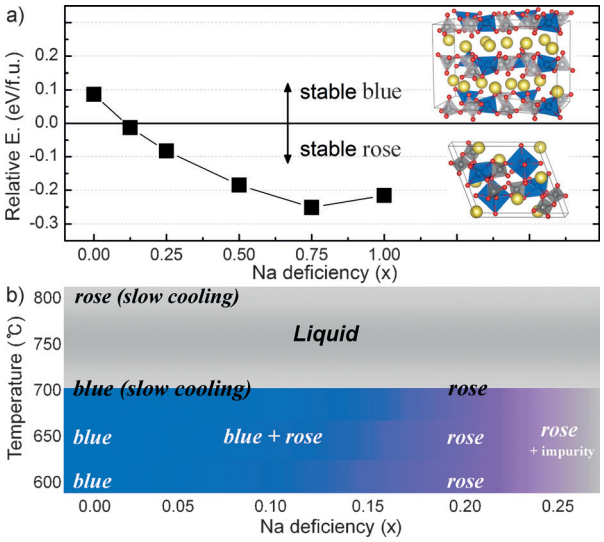

Figure 1. a) Relative energies of the rose and blue polymorphs as a function of the Na deficiency in $Na_{2-x}CoP_2O_7$. Inset: Unit cell of the blue and rose phases. b) Synthesis map of $Na_{2-x}CoP_2O_7$ compounds obtained from the XRD data in Figure S1.

form is more stable than the rose form by 0.1 eV per formula unit (f.u.), which is consistent with the experimental observation that the blue form is preferentially produced for $Na_2CoP_2O_7$.[11,12] With an increase in Na vacancies, however, the Co rose phase becomes systematically stabilized, implying that the formation of Na vacancies is energetically more favorable in the Co rose phase than in the Co blue phase. This difference in the binding strength of the Na ions can be understood by considering a simple electrostatic model, which will be discussed below.

On the basis of these computational analyses and insight gained from the literature, we synthesized stoichiometric ($x=0$) and nonstoichiometric ($x>0$) compounds of $Na_{2-x}CoP_2O_7$ at a temperature range of 600 to 800 °C (Figure 1b). For the stoichiometric precursor ratio, the Co blue phase was obtained at 600–700 °C, with a small amount of the Co rose phase, whereas the rose compound was formed by heating to 800 °C followed by cooling of the melted sample to room temperature at a cooling rate of 1 °C min^{-1}. On the other hand, the pure Co rose phase was successfully produced by decreasing the amount of Na precursor to $x=0.2$ in $Na_{2-x}CoP_2O_7$, regardless of the synthesis temperature or the cooling conditions (1–10 °C min^{-1}). Moreover, for a fixed temperature of 650 °C, which is the highest temperature at which the sample can be maintained in the solid state, the rose phase was gradually formed with a decrease in the Na content, resulting in the formation of a well-defined rose phase at $x=0.2$, without any traces of the blue phase. These results confirm that the Na deficiencies indeed stabilize the Co rose phase over its blue polymorph, as hypothesized and predicted by the electronic-structure calculations. For further structural and electrochemical studies, we removed the impurity phases in the $x=0.2$ sample, namely the rose nonstoichiometric form (RN), by using an excess of Co (see the Supporting Information for details).

To identify the structure and to understand the role of the Na deficiencies in the synthesized rose compounds, the X-ray diffraction (XRD) pattern of the RN sample was analyzed by Rietveld refinement[10f,16] (see Figure S2 and Tables S2–S4 for details). When comparing the refined RN structure (Figure 2a, left) to the non-defective crystal (Figure 2a, right), three differences are noticeable. First, the RN sample has a Na deficiency in the small tunnel along the c axis, denoted as site S1 in Figure 2a. Second, one identical Na position at the S1 site in the non-defective crystal splits into three subsites in the sodium-deficient samples. Third, the additional Co atoms then occupy the specific site S2 in Figure 2a by replacing Na, resulting in the chemical formula $Na_{1.63}Co_{1.13}P_2O_7$, which is

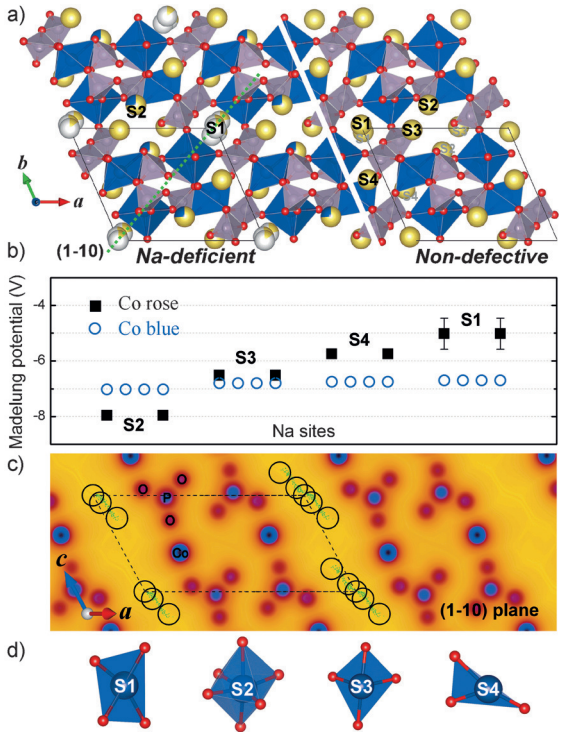

Figure 2. a) Refined sodium-deficient crystal structure of the synthesized Co rose phase (left) and a hypothetical Co rose phase without defects (right). Co blue, Na yellow, O red, P gray, vacancies white. b) Madelung potentials at each Na site of the rose and blue phases. c) Electrostatic potential map of the Co rose phase along the (1–10) plane, in which the light region is stable for Na^+ ions. The dashed line indicates the unit cell, and the black circles are disordered Na positions. The green dots are the most probable Na^+ positions obtained from the MC simulations. d) Oxygen coordination modes of Co upon substituting for Na at each site.

consistent with the compositional analysis (Table S5). The details of these differences are as follows:

1) The preferential formation of Na vacancies at the S1 site can be briefly explained by considering the Madelung potential because the Na ions are almost fully ionized, and thus their binding nature is mainly electrostatic.[17] Figure 2b shows the Madelung potential for each Na site for the rose and blue phases (see the Supporting Information for details); Na^+ ions generally experience a weaker potential in the Co rose phase than in the Co blue phase. S1 is a particularly unfavorable site for Na^+ ions, promoting the formation of Na vacancies at this site before any other positions are left vacant. The significant difference in Na stability between the rose and blue phases causes the Co rose phase to be preferentially formed under sodium-deficient conditions.
2) While partial Na vacancies are formed at S1, the remaining Na^+ ions in the small tunnel occupy three different crystallographic sites (see Figure 2a and Table S3). Figure 2c provides an electrostatic potential map across the (1–10) plane of the Co rose phase, which penetrates the center of the small tunnel (dashed line in Figure 2a). Along the *c* axis of this tunnel, the potential is extremely flat, allowing the occupation of multiple Na positions with similar stability, as indicated by the black circles in Figure 2c. These disordered sites match well with the most probable Na intercalation sites identified by Monte Carlo simulations (green dots in Figure 2c). Similar Na disordering has also been reported for other rose compounds.[16,18] Such ionic disorder in energetically degenerate sites is entropically favorable.
3) To maintain charge neutrality in the presence of Na^+ vacancies, some of the Co^{2+} ions should be oxidized to Co^{3+} or additional Co^{2+} ions should be introduced at related positions. Of these two possibilities for charge compensation, the nickel- and magnesium-based rose compounds are expected to prefer the addition of extra Ni or Mg atoms because they strongly favor the 2+ oxidation state.[16,18] On the other hand, in the iron-based rose compound, excess Fe^{2+} and oxidized Fe^{3+} states were both identified with Na vacancies as Fe can adopt both the 2+ and 3+ oxidation state.[10c–e] Based on the present refinement results, the Co rose phase also contains both Co^{3+} cations (8% of the total number of Co atoms for charge neutrality) and excess Co^{2+} ions, as in the Fe case. Among the six Na sites in the refined structure, only the S2 site has a typical octahedral coordination that is suitable for Co^{2+} and Co^{3+} as shown in Figure 2d,[19] whereas all other sites have distorted (S3 and S4) or planar (S1) local geometries with three to five oxygen ligands, and are unfavorable for Co occupation (Figure 2d). Therefore, the introduction of excess Co is expected to occur site-specifically at S2, leading to disorder between the Na and Co atoms.

The three differences arising from the nonstoichiometry consistently influence the phase stability of the rose compound: The formation enthalpy difference for Na vacancies in the rose and blue phases primarily results in the preferential formation of the rose form, whereas the latter two disorders (Na vacancies and Na/Co disorder) also contribute to the stabilization of the rose form by increasing the entropy. Interestingly, such nonstoichiometric compounds with deficient sodium and excess metal have also been observed for other rose-structured materials, such as $Na_{1.66}Fe_{1.17}P_2O_7$, $Na_{1.82}Ni_{1.09}P_2O_7$, and $Na_{1.82}Mg_{1.09}P_2O_7$,[10c,e,16,18] supporting our hypothesis that the lack of Na assists in the formation of the rose phases. Furthermore, in our rose samples, as well as in previously reported rose compounds,[10a] a small amount of sodium phosphates ($Na_4P_2O_7$ and/or $NaPO_3$) was present (Figure S1 and S2). We expect that such sodium impurities, aside from Na evaporation, lead to the depletion of Na and an excess of Co in the synthesized rose compounds.

The electrochemical properties of the Co rose phase were analyzed for the first time and compared with those of Co blue and Fe rose phases (Figure 3a). The RN sample exhibited a reversible capacity of approximately 80 mAh g^{-1},

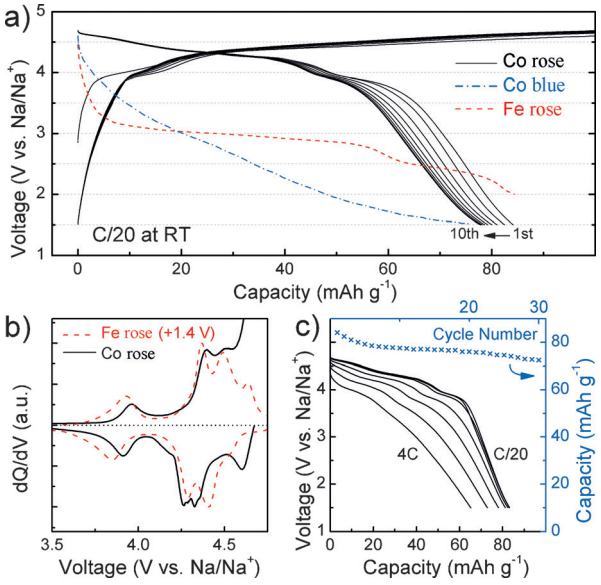

Figure 3. a) Galvanostatic cycles of the Co rose (RN), Fe rose, and Co blue polymorphs (from Ref. [20]). b) Differential capacity curves of the Fe- and Co-based rose polymorphs for each second cycle. The curve of the Fe rose polymorph was shifted by 1.4 V for comparison. c) Discharge curves at rates of C/20, C/10, C/5, C/2, 1C, 2C, and 4C, respectively, from right to left. Right axis: Cycle performance at a scan rate of C/10.

which corresponds to the operation of 0.84 Na ions per formula unit. The slightly lower capacity relative to the theoretical value, 95 mAh g^{-1}, is probably due to the fact that the Na sites (S2 in Figure 2a) are partially occupied by excess Co. Please note that our samples were coated with graphite to improve the electrical conductivity, but its contribution to the total capacity by intercalation of Na or anions is minor as shown in Figure S3. According to a previous report, the Co blue phase also exhibits a capacity of approximately 80 mAh g^{-1}, but an average voltage of only 3.0 V vs. Na/Na^+, as indicated by the blue line in Figure 3a,[20] a value that is substantially lower than the commonly expected Co^{2+}/Co^{3+}

redox potentials.[19] The authors ascribed this to the inferior crystal structure of the blue phase (Figure 1a, inset), in which the tetrahedral coordination of the Co centers leads to strong covalency and thus a low voltage. In remarkable contrast, the Co rose phase obtained in this work displayed an average voltage of 4.3 V vs. Na/Na^+, delivering an increase in energy density of more than 40% compared to its blue polymorph (344 vs. 240 $Wh\,kg^{-1}$). The origin of this voltage difference is not yet fully understood and requires further investigations (Figure S4).

The voltage profile of the Co rose material consists of one relatively low voltage plateau at 3.95 V and two higher voltage plateaus at 4.33 V and 4.43 V, as can be seen in the differential capacity curve in Figure 3b. This voltage profile, including the peak shape and intervals, matches well with that of the Fe-based rose compound (shifted by 1.4 V, red dashed line in Figure 3b), suggesting that the cell voltage was increased by as much as 1.4 V upon changing the TM center from Fe to Co while the operation mechanisms were maintained. This average voltage of 4.3 V vs. Na/Na^+ is nearly at the upper limit of the stable window of current SIB electrolytes. Indeed, the low coulombic efficiency observed in Figure 3b indicates that electrolyte decomposition occurred during the charge process, suggesting that a suitable electrolyte is necessary for the practical use of this material. Also, it is noteworthy that when building a full cell with electrodes made from the nonstoichiometric material, careful mass balancing between the anode and cathode is necessary not to lose the overall energy density. The reversible capacity is preserved at a discharging rate of up to C/5, as shown in Figure 3c, but moderate capacity fading was observed in faster operations. In a cycle performance test at C/10, the discharge capacity had decreased to 86% of its initial value after 30 cycles (Figure 3c, right axis).

In summary, we have shown that the introduction of Na deficiencies stabilizes the rose form of $Na_2CoP_2O_7$ over its other polymorphs, significantly simplifying its conventional synthetic conditions and routes. This rose-colored material exhibits stable cycling with an average voltage of 4.3 V vs. Na/Na^+, providing an improved energy density compared to its blue polymorph. These results demonstrate that the electrochemical properties of electrode materials can be markedly improved just by changing their crystal structure, and in the control of this polymorphism, nonstoichiometric factors such as alkali ion vacancies can play a pivotal role. We expect that the concepts and strategies proposed in this work, that is, the nonstoichiometry-driven control of polymorphism, can be generally applied for the development of new materials for various applications beyond battery electrodes.

Acknowledgements

This research was supported by the National Research Foundation funded by the Korea government (NRF-2014R1A4A1003712, NRF-2010-C1AAA001-0029031). H.K. thanks the KBSI (C36270) and the R&D Convergence Program of the National Research Council of Science & Technology (CAP-15-02-KBSI).

Keywords: crystal engineering · density functional calculations · nonstoichiometry · polymorphism · sodium-ion batteries

How to cite: *Angew. Chem. Int. Ed.* **2016**, *55*, 6662–6666
Angew. Chem. **2016**, *128*, 6774–6778

[1] a) M. S. Islam, C. A. J. Fisher, *Chem. Soc. Rev.* **2014**, *43*, 185–204; b) V. Palomares, M. Casas-Cabanas, E. Castillo-Martinez, M. H. Han, T. Rojo, *Energy Environ. Sci.* **2013**, *6*, 2312–2337; c) H. Pan, Y.-S. Hu, L. Chen, *Energy Environ. Sci.* **2013**, *6*, 2338–2360; d) M. D. Slater, D. Kim, E. Lee, C. S. Johnson, *Adv. Funct. Mater.* **2013**, *23*, 947–958; e) N. Yabuuchi, K. Kubota, M. Dahbi, S. Komaba, *Chem. Rev.* **2014**, *114*, 11636–11682.

[2] a) Y. Kawabe, N. Yabuuchi, M. Kajiyama, N. Fukuhara, T. Inamasu, R. Okuyama, I. Nakai, S. Komaba, *Electrochem. Commun.* **2011**, *13*, 1225–1228; b) F. Sauvage, E. Quarez, J.-M. Tarascon, E. Baudrin, *Solid State Sci.* **2006**, *8*, 1215–1221.

[3] a) M. Nose, H. Nakayama, K. Nobuhara, H. Yamaguchi, S. Nakanishi, H. Iba, *J. Power Sources* **2013**, *234*, 175–179; b) C. S. Park, H. Kim, R. A. Shakoor, E. Yang, S. Y. Lim, R. Kahraman, Y. Jung, J. W. Choi, *J. Am. Chem. Soc.* **2013**, *135*, 2787–2792.

[4] a) P. Barpanda, G. Oyama, S.-i. Nishimura, S.-C. Chung, A. Yamada, *Nat. Commun.* **2014**, *5*, 4358; b) S. Y. Lim, H. Kim, J. Chung, J. H. Lee, B. G. Kim, J.-J. Choi, K. Y. Chung, W. Cho, S.-J. Kim, W. A. Goddard, Y. Jung, J. W. Choi, *Proc. Natl. Acad. Sci. USA* **2014**, *111*, 599–604.

[5] M. Saubanère, M. B. Yahia, S. Lebègue, M.-L. Doublet, *Nat. Commun.* **2014**, *5*, 5559.

[6] a) P. Barpanda, M. Ati, B. C. Melot, G. Rousse, J.-N. Chotard, M.-L. Doublet, M. T. Sougrati, S. A. Corr, J.-C. Jumas, J.-M. Tarascon, *Nat. Mater.* **2011**, *10*, 772–779; b) R. Tripathi, G. Popov, B. L. Ellis, A. Huq, L. F. Nazar, *Energy Environ. Sci.* **2012**, *5*, 6238–6246.

[7] a) M. E. Arroyo-de Dompablo, R. Dominko, J. M. Gallardo-Amores, L. Dupont, G. Mali, H. Ehrenberg, J. Jamnik, E. Moran, *Chem. Mater.* **2008**, *20*, 5574–5584; b) A. Boulineau, C. Sirisopanaporn, R. Dominko, A. R. Armstrong, P. G. Bruce, C. Masquelier, *Dalton Trans.* **2010**, *39*, 6310–6316.

[8] L. Lander, M. Reynaud, G. Rousse, M. T. Sougrati, C. Laberty-Robert, R. J. Messinger, M. Deschampps, J.-M. Tarascon, *Chem. Mater.* **2014**, *26*, 4178–4189.

[9] a) C. Parada, J. Perles, R. Saez-Puche, C. Ruiz-Valero, N. Snejko, *Chem. Mater.* **2003**, *15*, 3347–3351; b) A. Saracibar, A. Van der Ven, M. E. Arroyo-de Dompablo, *Chem. Mater.* **2012**, *24*, 495–503; c) D.-H. Seo, H. Kim, I. Park, J. Hong, K. Kang, *Phys. Rev. B* **2011**, *84*, 220106.

[10] a) P. Barpanda, T. Ye, S.-i. Nishimura, S.-C. Chung, Y. Yamada, M. Okubo, H. Zhou, A. Yamada, *Electrochem. Commun.* **2012**, *24*, 116–119; b) C.-Y. Chen, K. Matsumoto, T. Nohira, R. Hagiwara, *J. Electrochem. Soc.* **2014**, *162*, A176–A180; c) K.-H. Ha, S. H. Woo, D. Mok, N.-S. Choi, Y. Park, S. M. Oh, Y. Kim, J. Kim, J. Lee, L. F. Nazar, K. T. Lee, *Adv. Energy Mater.* **2013**, *3*, 770–776; d) H. Kim, R. A. Shakoor, C. Park, S. Y. Lim, J.-S. Kim, Y. N. Jo, W. Cho, K. Miyasaka, R. Kahraman, Y. Jung, J. W. Choi, *Adv. Funct. Mater.* **2013**, *23*, 1147–1155; e) Y. Niu, M. Xu, C. Cheng, S.-J. Bao, J. Hou, S. Liu, F. Yi, H. He, C. M. Li, *J. Mater. Chem. A* **2015**, *3*, 17224–17229; f) P. Barpanda, G. Liu, C. D. Ling, M. Tamaru, M. Avdeev, S.-C. Chung, Y. Yamada, A. Yamada, *Chem. Mater.* **2013**, *25*, 3480–3487.

[11] P. Barpanda, M. Avdeev, C. D. Ling, J. Lu, A. Yamada, *Inorg. Chem.* **2013**, *52*, 395–401.

[12] F. Erragh, A. Boukhari, B. Elouadi, E. M. Holt, *J. Crystallogr. Spectrosc. Res.* **1991**, *21*, 321–326.

[13] a) E.-S. Lee, A. Huq, H.-Y. Chang, A. Manthiram, *Chem. Mater.* **2012**, *24*, 600–612; b) M. Lengyel, G. Atlas, D. Elhassid, X. Zhang, I. Belharouak, R. L. Axelbaum, *J. Electrochem. Soc.*

2014, *161*, A1023 – A1031; c) J. Xiao, N. A. Chernova, M. S. Whittingham, *Chem. Mater.* **2008**, *20*, 7454 – 7464.
[14] a) N. S. Bell, C. Edney, J. S. Wheeler, D. Ingersoll, E. D. Spoerke, *J. Am. Ceram. Soc.* **2014**, *97*, 3744 – 3748; b) Y. H. Jung, A. S. Christiansen, R. E. Johnsen, P. Norby, D. K. Kim, *Adv. Funct. Mater.* **2015**, *25*, 3227 – 3237; c) R. Shanmugam, W. Lai, *J. Electrochem. Soc.* **2015**, *162*, A8 – A14.
[15] G. Kresse, J. Furthmüller, *Comput. Mater. Sci.* **1996**, *6*, 15 – 50.
[16] F. Erragh, A. Boukhari, F. Abraham, B. Elouadi, *J. Solid State Chem.* **2000**, *152*, 323 – 331.
[17] H. Kim, Y. Jung, *Int. J. Quantum Chem.* **2015**, *115*, 1141 – 1146.
[18] G. Liu, S.-i. Nishimura, S. C. Chung, K. Fujii, M. Yashima, A. Yamada, *J. Mater. Chem. A* **2014**, *2*, 18353 – 18359.
[19] G. Hautier, A. Jain, S. P. Ong, B. Kang, C. Moore, R. Doe, G. Ceder, *Chem. Mater.* **2011**, *23*, 3495 – 3508.
[20] P. Barpanda, J. Lu, T. Ye, M. Kajiyama, S.-C. Chung, N. Yabuuchi, S. Komaba, A. Yamada, *RSC Adv.* **2013**, *3*, 3857 – 3860.

Received: January 29, 2016
Published online: April 21, 2016

